JOURNAL OF MATERIALS SCIENCE 28 (1993) 2706–2714

The normalized numbers of grain boundaries, triple points and growth fronts in a circular growing two-dimensional Voronoi tessellation with Poisson-distributed nuclei

G. E. W. SCHULZE, L. O. SCHWAN*
*Abteilung für Werkstoffwissenschaft and *Lehrstuhl für Festkörperspektroskopie, Institut für Physik der Kondensierten Materie, Heinrich-Heine-Universität Düsseldorf, Universitätsstrasse 1, Gebiet 25.23.01, W-4000 Düsseldorf, Germany*

The topological properties of a set of nuclei undergoing a phase transformation were investigated. The nuclei were spread out in a plane according to a Poisson distribution. All centres started to grow at the same moment and with the same constant rate. They grew circularly and free of shrinking. The mean numbers per nucleus of grain boundaries, triple points and growth fronts were calculated as functions of the degree of transformation, F ($0 \leqslant F \leqslant 1$). For these relationships we deduce plain and exact expressions.

1. Introduction and aims

1.1. Model

The mathematical model used is a plane with Poisson-distributed points. The points represent the nuclei. All nuclei start to transform at the same moment. They grow circularly and with the same constant rate. They grow free of shrinking. The growth may be a solidification, crystallization, recrystallization or phase transformation. If two circular growth fronts impinge, a straight grain boundary is formed. The grain boundary bisects perpendicularly the line between both centres. Each grain boundary ends in two triple points as shown in Fig. 1 or Fig. 3.

The triple points that are formed by the intersection of three curves are divided into static and dynamic triple points. The static triple points are immobile and are formed by the ends of three grain boundaries. The dynamic triple points are moving and are formed by the end of a grain boundary and the ends of two growth fronts.

Fig. 1 shows a "Poisson-distributed growing two-dimensional Voronoi tessellation" which is also called the "growing two-dimensional cell model". The degree of growth, F ($0 \leqslant F \leqslant 1$), is $F = 0.6$. This means that 60% of the plane is transformed and 40% of the plane is still in the initial state. For degree of growth we also use the terms fraction solidified, fraction crystallized, fraction recrystallized or degree of transformation.

Fig. 1 shows two phases: the growing phase and the disappearing phase. The transformation begins with a large number of small "islands". With increasing F the islands combine into larger aggregates and their number decreases. Finally, at $F = 1$ only one gigantic island remains. On the other hand, there is a gigantic "sea" at the beginning, when $F = 0$, which is subdivided into smaller seas during the transformation which are finally exhausted at $F = 1$. The "islands" are convex and the "seas" concave, always with the same radius, R, for a given F.

Fig. 1 shows the nuclei as points; the grain boundaries as straight lines that end in the triple points; the static triple points as the ends of three straight lines; the dynamic triple points as the end of one straight line and the ends of two arcs; and the growth fronts as circles and arcs, all with the same radius of growth, R. Fig. 1 shows further that the grain boundaries are divided into types 1, 2 and 3: type 1 ends at two dynamic triple points, type 2 ends at one static and one dynamic triple point and type 3 ends at two static triple points.

Furthermore, Fig. 1 shows that the grain boundaries and the static triple points are embedded in the growing phase. The growth fronts and the dynamic triple points, however, lie at the phase boundaries.

1.2. Experiment

Fig. 2 shows the experimental realization of this model. It shows a microphotograph of a foil of polypropylene 4 μm thick after the following heat-treatment: first the foil was melted, then it was temporarily cooled to form nuclei, and then it was again heated to the growth temperature, T. This temperature (T) lay below the melting temperature. Therefore, the foil was in an undercooled liquid state. Out of the nuclei mature spherulites grow at T, but new nuclei are not formed. If two neighbouring spherulites touch, a straight grain boundary begins to form.

The growing spherulitic microstructure is marked [1] in equal time intervals, shown by the circles and

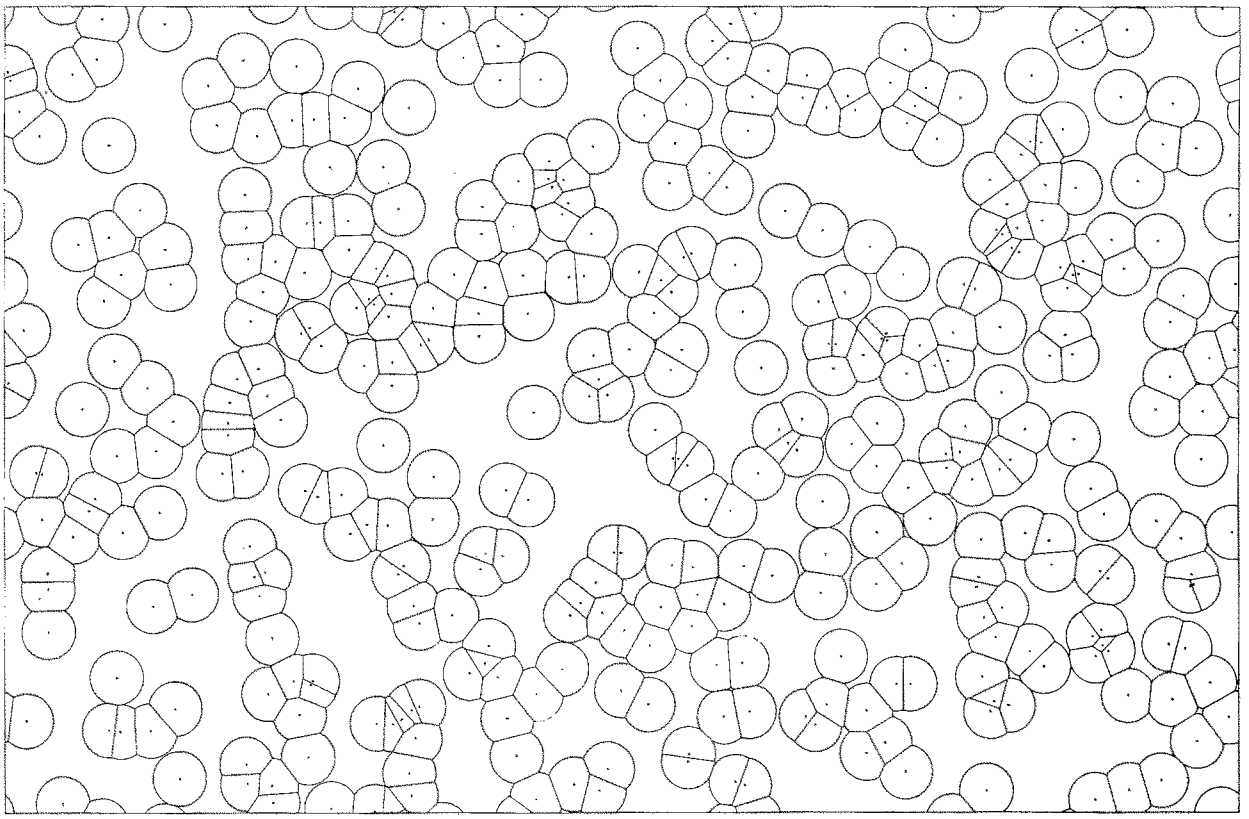

Figure 1 400 nuclei shown as points that are Poisson-distributed. For these a two-dimensional Voronoi tessellation is shown at $F = 0.6$. The numbers of ten properties were counted: the grain boundaries of type 1 (161), type 2 (286), type 3 (127) and of the sum of all three types (574); the dynamic (608), static (180) and all triple points (788); the circles (9), arcs (608) and all growth fronts (617). These numbers were divided by 400 in order to obtain the values of one nucleus.

the arcs in Fig. 2. Finally, if the foil is perfectly primary crystallized, a photograph such as that shown in Fig. 2 is obtained at room temperature. It conforms to a "growing two-dimensional Voronoi tessellation". The Poisson distribution of the nuclei cannot be identified from Fig. 2, since the number of nuclei is too small. However, we experimentally manifested the Poisson distribution by the use of 1778 nuclei [2].

1.3. Basic relationships

Two basic relationships used in this work, the Poisson distribution and the Avrami relationship, are briefly introduced. We choose in this paper the area that contains on average one nucleus as the unit area. Since the nuclei are Poisson-distributed, the relative number, p_k, to find k nuclei in the area x [3] is

$$p_k(x) = (x^k/k!)\exp(-x) \quad (1)$$

with $k = 0, 1, 2, \ldots; x > 0$; and $\sum_{k=0}^{\infty} p_k(x) = 1$.

Since the Poisson-distributed nuclei start to grow at the same moment and since they grow circularly, the dependence of F on R is given by an Avrami relationship [4]

$$F(R) = 1 - \exp(-\pi R^2) \quad \text{for } R \geqslant 0 \quad \text{and} \quad 0 \leqslant F \leqslant 1 \quad (2)$$

The constant growth rate, v, is given by $v = R/t$, where t is the time of growth. Of course, we can substitute $R = vt$. We choose in this paper $v = 1$. Then we obtain the values listed in Table I.

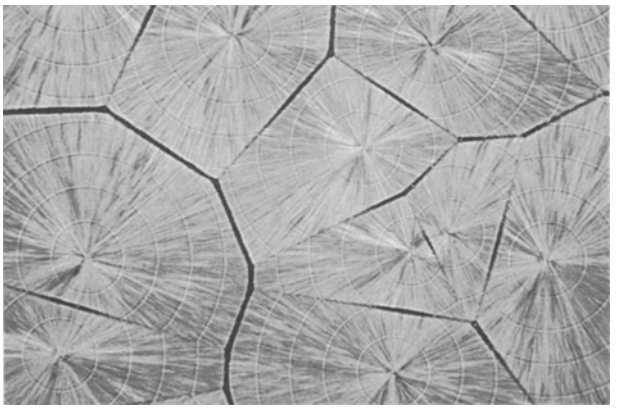

Figure 2 Micrography of a foil of polypropylene 4 μm thick showing the "model" at $F = 1$. Circles and arcs show the growth fronts at four time-points. Three neighbouring nuclei form a static triple point. The distance of these three nuclei from the static triple point is the same.

TABLE I

F	R
0	0
0.2	0.266 51
0.4	0.403 24
0.6	0.540 06
0.8	0.715 75
0.9	0.856 11
0.99	1.210 73
0.999	1.482 80
1	∞

1.4. Normalization

The number of all grain boundaries (or other properties) that are found in the transforming two-dimensional Voronoi tessellation of Poisson-distributed nuclei depends on the number of nuclei (N) and t, R or F.

For example, take $N = 10^5$ and $F = 0.6$. Then we count all grain boundaries (or other properties). We did so three times because of the fluctuations and we obtained 143 125, 143 079 and 143 080. Normalized to one nucleus the numbers of all grain boundaries are 1.431 25, 1.430 79 and 1.430 80. The fluctuating values become more similar as N increases. Finally, at $N \to \infty$ we have one exact value. This is the mean normalized number of all grain boundaries for $N \to \infty$ and $F = 0.6$. It amounts to 1.433 48 . . . and in this paper is called the "normalized number" for short.

We note that the result of the theory of probability also gives this "normalized number."

1.5. Aims

From both basic equations and by means of probability theory we deduce the normalized numbers in dependence on R and the normalized numbers in dependence on the degree of growth, F, of: grain boundaries of types 1, 2 and 3, and the sum of all three types, called $T_{\text{type 1}}$, $T_{\text{type 2}}$, $T_{\text{type 3}}$ and T_{total}, respectively; dynamic, static and all triple points, called U_{dyn}, U_{static} and U_{total}, respectively; and circles, arcs and all growth fronts, called V_{circles}, V_{arcs} and V_{total}, respectively.

We note that if the foil has N finite nuclei at F, then we have on average $NT_{\text{type 1}}(F), NT_{\text{type 2}}(F), \ldots, NV_{\text{total}}(F)$ numbers of grain boundaries of type $1, 2, \ldots$, and of all growth fronts, respectively.

Three years ago we investigated the model along an (infinite) straight line, named the Rosiwal traverse [5, 6].

2. Normalized numbers of grain boundaries in dependence on R

In the produced microstructure with a radius of growth R, we have well-defined mean values per nucleus (or per unit area) for the number of grain boundaries of types 1, 2 and 3, and of the sum of all types. These relationships are deduced from probability theory in the following.

2.1. Normalized number of grain boundaries of type 1 in dependence on R

A nucleus (A) is a fixed starting point of our consideration. A second nucleus (B) is encountered at a distance $2Y$. Since the points are Poisson-distributed, the probability of finding one point in the area element $2\pi(2Y)\,dY$ is given by

$$p_1(Y)\,dY = \frac{[2\pi(2Y)\,dY]^1}{1!} \exp[-2\pi(2Y)\,dY]$$

The expansion in a power series and rupture after the first term gives

$$p_1(Y)\,dY = 4\pi Y\,dY \qquad (3)$$

A grain boundary of type 1 forms the bisecting line between the two nuclei A and B. The end-points of the grain boundary are designated C and C′ in Fig. 3. C and C′ are the points of intersection of the two circles with radius of growth R from the nuclei A and B. Of course, $0 \leqslant Y \leqslant R$, and at C and C′ lie dynamic triple points. The distance $\overline{CC'}$ is denoted as b. It holds that

$$b = 2(R^2 - Y^2)^{1/2} \qquad \text{for } 0 \leqslant Y \leqslant R$$

$b(Y, R)$ exists if no nucleus lies in the ∞-shaped region of Fig. 4. (A nucleus within the ∞-shaped region would reach b before a grain boundary of type 1 could exist, but this conflicts with the assumption.) The area (S) of the ∞-shaped region is easily computed as

$$S(Y, R) = 2\pi R^2 - 2R^2\{\arcsin(Y/R) - (Y/R)[1 - (Y/R)^2]^{1/2}\} \qquad (4)$$

for $0 \leqslant Y \leqslant R$. The probability of finding no nucleus in the area S is for Poisson-distributed nuclei

$$p_0(S) = (S^0/0!)\exp(-S) = \exp(-S)$$

The probability, $T_{\text{type 1}}(Y, R)\,dY$, of finding at a distance between $2Y$ and $2Y + dY$ from a given nucleus

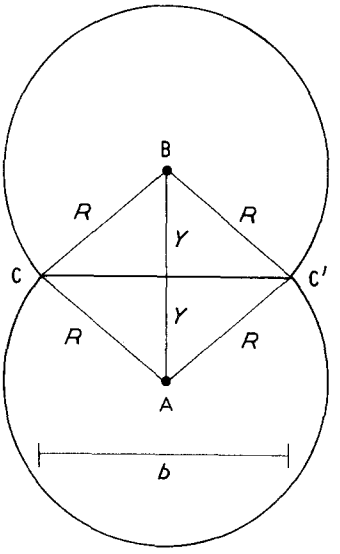

Figure 3 Between two nuclei A and B there is a distance of $2Y$. At a radius of growth R the spherulites form a grain boundary of type 1 with length b. C and C′ are two dynamic triple points.

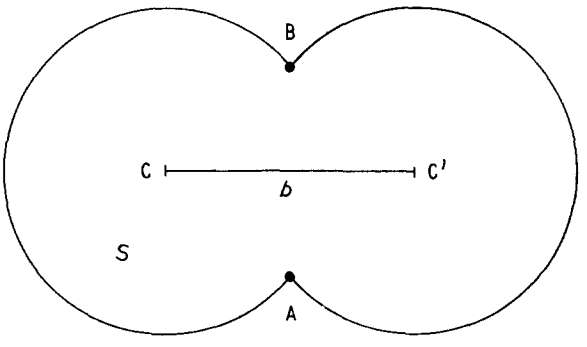

Figure 4 The same state as in Fig. 3. The ∞-shaped region must not contain any nucleus except A and B on the border.

A a second nucleus B, and of finding simultaneously a grain boundary of type 1, is found by multiplication because of the independence of the events. The probability is

$$T_{\text{type 1}}(Y, R)\,dY = p_1(Y, R)\,dY\,p_0(S) = 4\pi Y \exp(-S)\,dY \quad (5)$$

Integrating from $Y = 0$ to R, $T_{\text{type 1}}(R)$ is obtained

$$T_{\text{type 1}}(R) = \int_{Y=0}^{R} 4\pi Y \exp[-S(Y, R)]\,dY \quad (6)$$

$T_{\text{type 1}}(R)$ is the normalized number of grain boundaries of type 1 in dependence on R. $T_{\text{type 1}}(R)$ is calculated from Equations 4 and 6 by numerical integration. The result is shown graphically in Fig. 5.

2.2. Normalized number of grain boundaries of type 2 in dependence on R

The grain boundary of type 2a is limited to the left side of the nucleus A by a dynamic triple point and to the right side of the nucleus A by a static triple point. At the grain boundary of type 2b this is reversed. It holds that

$$T_{\text{type 2}}(R) = T_{\text{type 2a}}(R) + T_{\text{type 2b}}(R) = 2T_{\text{type 2a}}(R) \quad (7)$$

At first we regard type 2a and we start with the ∞-shaped region. The point C has to be a dynamic triple point, and therefore we have to find no nucleus in its circle with the radius of growth R. This probability is given by

$$4\pi Y\,dY \exp(-\pi R^2)$$

Fig. 6 shows the area S_{rest}, which is S minus πR^2. Within $S_{\text{rest}}(Y, R)$ there must be at least one nucleus in order to have a static triple point; otherwise this grain boundary is of type 1, and this may not be. The probability of finding no nucleus within the area S_{rest} is $\exp(-S_{\text{rest}})$. Therefore, the probability of finding any number of nuclei other than zero within area S_{rest} is $1 - \exp(-S_{\text{rest}})$. Collectively we have to multiply the independent probabilities

$$T_{\text{type 2a}}(Y, R)\,dY = 4\pi Y \exp(-\pi R^2)\{1 - \exp[-S_{\text{rest}}(Y, R)]\}\,dY \quad (8)$$

Integrating from $Y = 0$ to $Y = R$,

$$T_{\text{type 2a}}(R) = \int_{Y=0}^{R} 4\pi Y \exp(-\pi R^2)\,dY - \int_{Y=0}^{R} 4\pi Y \exp(-\pi R^2) \times \exp[-S_{\text{rest}}(Y, R)]\,dY \quad (9)$$

Since the areas

$$\pi R^2 + S_{\text{rest}}(Y, R) = S(Y, R)$$

upon integration Equation 9 gives

$$T_{\text{type 2a}}(R) = 2\pi R^2 \exp(-\pi R^2) - \int_{Y=0}^{R} 4\pi Y \exp[-S(Y, R)]\,dY \quad (10)$$

The integral equals $T_{\text{type 1}}(R)$ from Equation 6. From Equation 7 it holds from Equation 10 that

$$T_{\text{type 2}}(R) = 4\pi R^2 \exp(-\pi R^2) - 2T_{\text{type 1}}(R) \quad (11)$$

$T_{\text{type 2}}(R)$ is the mean number of grain boundaries of type 2 per nucleus. $T_{\text{type 2}}(R)$ is shown graphically in Fig. 5.

2.3. Normalized number of grain boundaries of type 3 in dependence on R

The grain boundaries of type 3 end between C and C′ in Fig. 3, without reaching C and C′. D in Fig. 7 is the

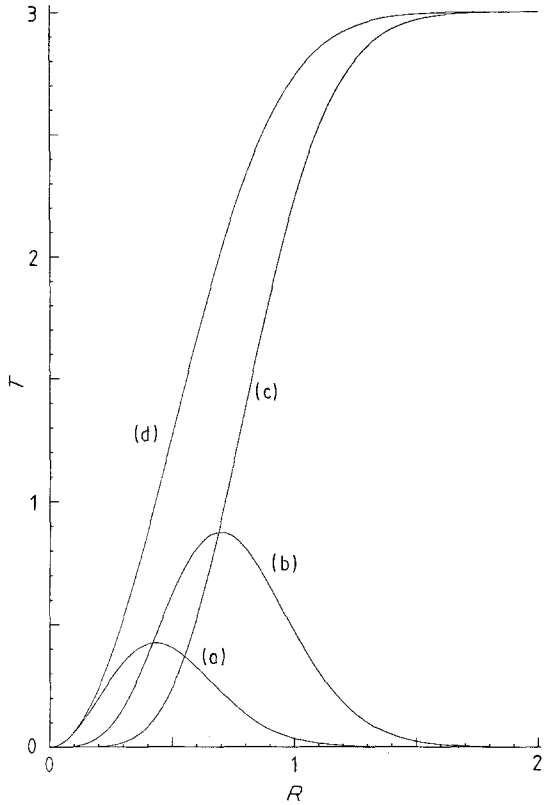

Figure 5 Graph of the normalized numbers of grain boundaries of types 1, 2 and 3, and the sum of all three types in dependence on R: (a) $T_{\text{type 1}}$, (b) $T_{\text{type 2}}$, (c) $T_{\text{type 3}}$ and (d) T_{total}.

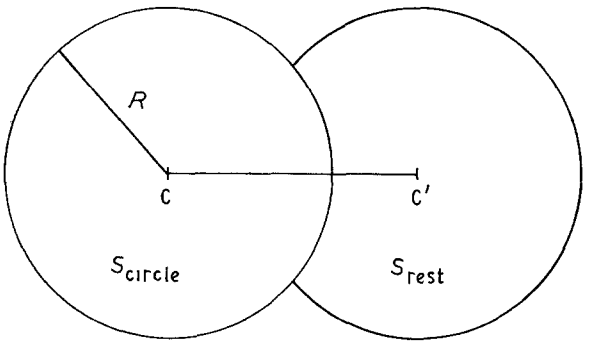

Figure 6 S_{circle} is a circular area around C with radius of growth R. It holds from Fig. 4 that $S_{\text{rest}} = S - S_{\text{circle}}$. Within the region S_{rest} there is at least one nucleus if the construction is valid for a grain boundary of type 2a.

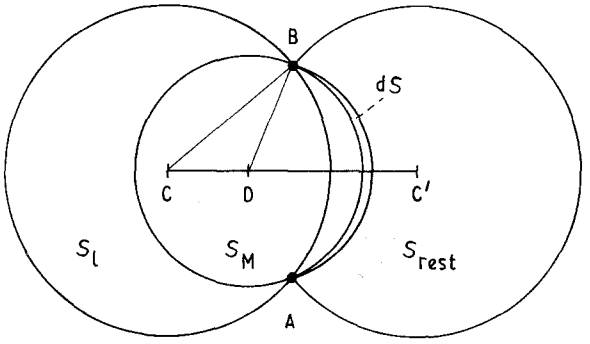

Figure 7 Construction of the areas used for the calculation of grain boundaries of type 3. All four circles or arcs hit the nuclei A and B. The neighbouring nucleus on the right-hand side is arranged in the differential area element dS within S_{rest}.

right end-point of the grain boundary, if the circle around D which goes through A and B has the circle area of S_M. The probability of finding no nucleus within S_M is $\exp(-S_M)$. D is also the right end-point if within the area element dS on the right-hand side of the circle S_M there is not less than one nucleus. The probability is $[1 - \exp(-\mathrm{d}S)]$. This equals dS because of the expansion in a power series and rupture after the second term.

The left end of the grain boundary lies between C and D. The probability of finding not less than one nucleus within the region S_I in Fig. 7 amounts to $[1 - \exp(-S_I)]$. The three independent probabilities have to be multiplied

$$\exp(-S_M)[1 - \exp(-S_I)]\,\mathrm{d}S \qquad (12)$$

D can occupy any position from C to C'. This means that the area element dS has to be integrated over S_{rest}

$$T_{type\,3}(R) = \int_{S_{rest}} \exp(-S_M)[1 - \exp(-S_I]\,\mathrm{d}S \qquad (13)$$

The result of the numerical integration is shown graphically in Fig. 5.

As shown in Fig. 5, $T_{type\,3}(R \to \infty) = 3$. This behaviour means that an average of three grain boundaries belong to one nucleus. The following interpretation is possible: each polygon around one nucleus has six sides an average [7]. This is understandable since each grain boundary has two nuclei, A and B.

2.4. Normalized number of all grain boundaries in dependence on R

The normalized number of all grain boundaries in dependence on R, $T_{total}(R)$, is

$$T_{total}(R) = T_{type\,1}(R) + T_{type\,2}(R) + T_{type\,3}(R) \qquad (14)$$

Inserting $T_{type\,1}(R)$ from Equation 16 (below) and $T_{type\,3}(R)$ from Equation 18 (below) into Equation 14

$$T_{total}(R) = \tfrac{1}{2}[U_{dyn}(R) - T_{type\,2}(R)] + T_{type\,2}(R) + \tfrac{1}{2}[3U_{static}(R) - T_{type\,2}(R)]$$

The $T_{type\,2}(R)$ cancels out and we obtain from Equations 17 and 19 (below) that

$$\begin{aligned} T_{total}(R) &= 2\pi R^2 \exp(-\pi R^2) \\ &\quad + 3[1 - \exp(-\pi R^2)] \\ &\quad - 3\pi R^2 \exp(-\pi R^2) \\ &= 3[1 - \exp(-\pi R^2)] \\ &\quad - \pi R^2 \exp(-\pi R^2) \end{aligned} \qquad (15)$$

$T_{total}(R)$ is a Veuuch analytical expression and it is shown graphically in Fig. 5.

3. Normalized numbers of triple points in dependence on R

In previous work we found the mean numbers by numerical integration. Here we find the numbers of triple points by exact integration [8].

3.1. Normalized number of dynamic triple points in dependence on R

The normalized number of dynamic triple points in dependence on R equals 2 for grain boundaries of type 1 and equals 1 for grain boundaries of type 2. Therefore, the normalized number, $U_{dyn}(R)$, of dynamic triple points in dependence on R is

$$U_{dyn}(R) = 2T_{type\,1}(R) + T_{type\,2}(R) \qquad (16)$$

With Equation 11 there is an exact analytical expression for $U_{dyn}(R)$

$$U_{dyn}(R) = 4\pi R^2 \exp(-\pi R^2) \qquad \text{for } R > 0 \qquad (17)$$

$U_{dyn}(R)$ is shown graphically in Fig. 8. It holds that

$$\int_{R=0}^{\infty} U_{dyn}(R)\,\mathrm{d}R = \int_{R=0}^{\infty} 4\pi R^2 \exp(-\pi R^2)\,\mathrm{d}R = 1$$

3.2. Normalized number of static triple points in dependence on R

Each static triple point contains three ends of grain boundaries. Therefore, we have to divide the number of grain boundaries involved by 3. The grain boundaries involved are of the types 2 and 3. The grain boundaries of type 2 have one and those of type 3 have two static triple points. Therefore, the normalized number of static triple points in dependence on R is

$$U_{static}(R) = \tfrac{1}{3}[T_{type\,2}(R) + 2T_{type\,3}(R)] \qquad (18)$$

$U_{static}(R)$ is shown graphically in Fig. 8. Fig. 8 shows that $U_{static}(R \to \infty) = 2$. This result says that in the completely transformed state there are two static triple points for each nucleus.

Another deduction given in the Appendix yields an exact analytical result for $U_{static}(R)$

$$U_{static}(R) = 2[1 - \exp(-\pi R^2) - \pi R^2 \exp(-\pi R^2)] \qquad (19)$$

Of course, Equations 18 and 19 are identical.

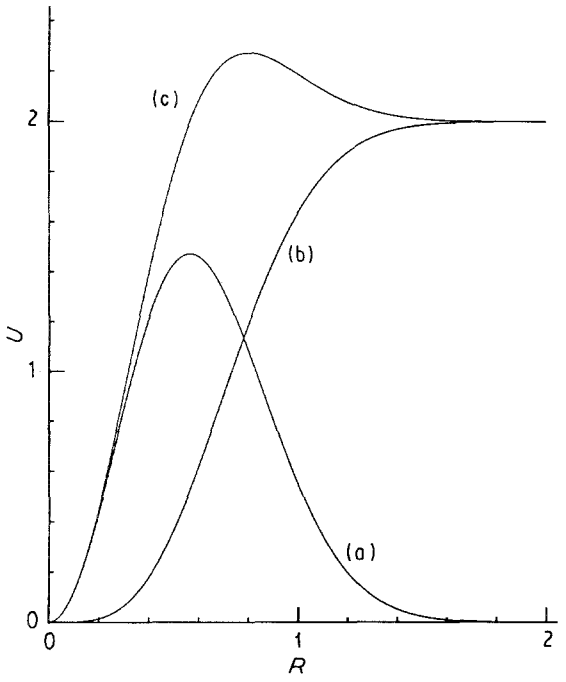

Figure 8 Graph of the normalized numbers of dynamic, static and all triple points in dependence on R: (a) U_{dyn}, (b) U_{static} and (c) U_{total}.

3.3. Normalized number of all triple points in dependence on R

The mean values for the sum of all triple points is given by $U_{total}(R)$

$$U_{total}(R) = U_{dyn}(R) + U_{static}(R) \quad (20)$$

$$= 4\pi R^2 \exp(-\pi R^2) + 2[1 - \exp(-\pi R^2) - \pi R^2 \exp(-\pi R^2)]$$

$$= 2[1 - \exp(-\pi R^2) + \pi R^2 \exp(-\pi R^2)] \quad (21)$$

$U_{total}(R)$ is shown in Fig. 8.

4. Normalized number of growth fronts in dependence on R

The growth fronts are either circles or arcs all with the same radius. We find again the normalized numbers of growth fronts in dependence on R by an exact deduction.

4.1. Normalized number of circles in dependence on R

First we deduce the normalized number of circles in dependence on R. The circles with radius R must not interfere with another nucleus. Therefore, a circle with the area $\pi(2R)^2$ must be free of nuclei. This gives for Poisson-distributed nuclei the relative number

$$V_{circles}(R) = \frac{[\pi(2R)^2]^0}{0!} \exp[-\pi(2R)^2]$$

$$= \exp(-4\pi R^2) \quad (22)$$

$V_{circles}(R)$ is shown graphically in Fig. 9.

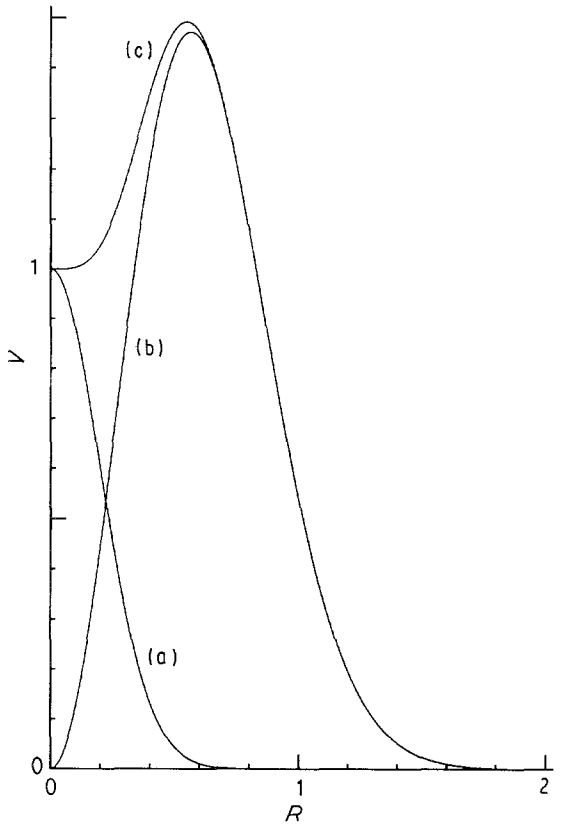

Figure 9 Graph of the normalized numbers of circles, arcs and all growth fronts in dependence on R: (a) $V_{circles}$, (b) V_{arcs} and (c) V_{total}.

4.2. Normalized number of arcs in dependence on R

The number of arcs equals the number of dynamic triple points. This result is unexpected. It is understandable if each dynamic triple point is identified by an arc that is placed to the right of the dynamic triple point. It holds that

$$V_{arcs}(R) = U_{dyn}(R) \quad (23)$$

$V_{arcs}(R)$ is shown in Fig. 9.

4.3. Normalized number of all growth fronts in dependence on R

Since the growth fronts contain circles and arcs, the normalized number of growth fronts in dependence on R, $V_{total}(R)$, is by addition

$$V_{total}(R) = V_{circles}(R) + V_{arcs}(R) \quad (24)$$

$$V_{total}(R) = \exp(-4\pi R^2) + 4\pi R^2 \exp(-\pi R^2) \quad (25)$$

$V_{total}(R)$ is shown graphically in Fig. 9.

5. Normalized numbers of all ten properties in dependence on F

So far we have used R in order to calculate the normalized numbers of the ten properties. Now we use F in order to calculate the normalized numbers of the ten properties. The transformation, $F(R)$, is given by Equation 2.

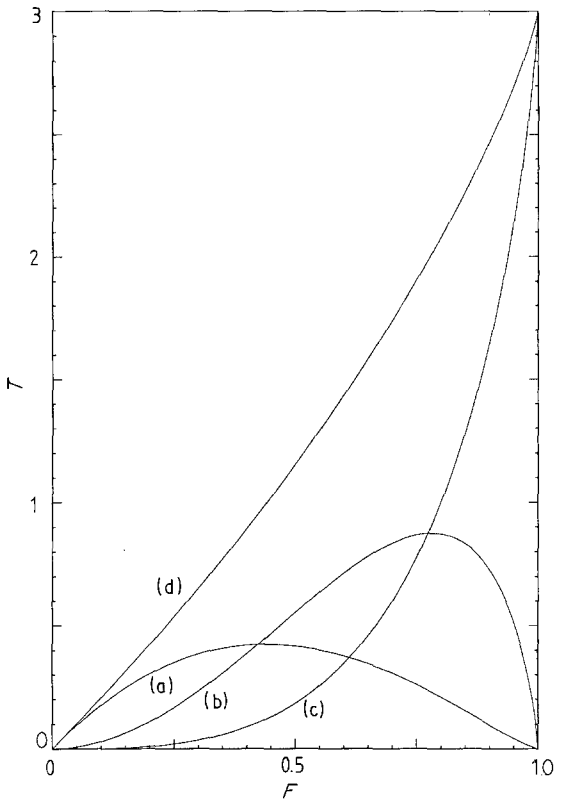

Figure 10 Graphical demonstration of the normalized numbers of grain boundaries of types 1, 2 and 3. and the sum of all three types in dependence on F: (a) $T_{\text{type 1}}$, (b) $T_{\text{type 2}}$, (c) $T_{\text{type 3}}$ and (4) T_{total}.

5.1. Normalized numbers of grain boundaries of types 1, 2 and 3 in dependence on F

Numerical integration yields $T_{\text{type 1}}(R)$ from Equation 6, $T_{\text{type 2}}(R)$ from Equation 11 and $T_{\text{type 3}}(R)$ from Equation 13. By means of the transformation $F(R)$ we obtain $T_{\text{type 1}}(F)$, $T_{\text{type 2}}(F)$ and $T_{\text{type 3}}(F)$. These are shown graphically in Fig. 10. The error of the numerical integration is $< 3‰$ and it is within the range of the thickness of the lines.

5.2. Normalized numbers of the seven remaining properties in dependence on F

The transformation of Equation 2, $F(R)$, yields

$$\exp(-\pi R^2) = 1 - F$$

$$\pi R^2 = -\ln(1 - F)$$

We multiply the two left-hand sides and then the two right-hand sides, obtaining

$$\pi R^2 \exp(-\pi R^2) = -(1 - F)\ln(1 - F)$$

$$= g(F) \qquad (26)$$

The expression $g(F)$ frequently appears and is shown in Fig. 11.

Now we consider the normalized numbers of $T_{\text{total}}(R)$ (Equation 15), $U_{\text{dyn}}(R)$ (Equation 17), $U_{\text{static}}(R)$ (Equation 19), $U_{\text{total}}(R)$ (Equation 21), $V_{\text{circles}}(R)$ (Equation 22), $V_{\text{arcs}}(R)$ (Equation 23) and $V_{\text{total}}(R)$ (Equation 25). All of these normalized numbers in dependence on R are exact analytical expressions. We transform these normalized numbers, which

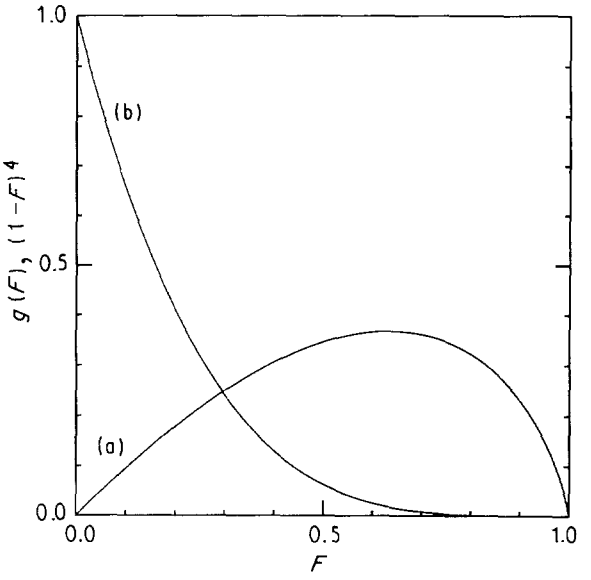

Figure 11 Graph of (a) $g(F)$ and (b) $(1 - F)^4$ for $0 \leqslant F \leqslant 1$.

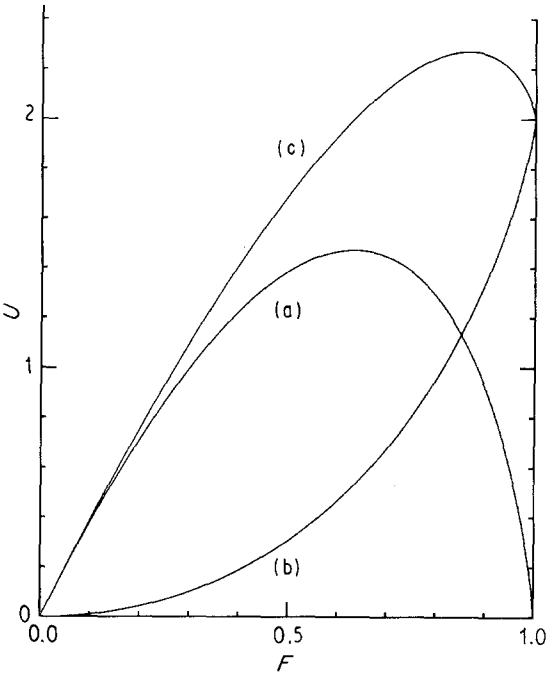

Figure 12 Graph of the normalized numbers of dynamic, static and all triple points in dependence on F: (a) U_{dyn}, (b) U_{static} and (c) U_{total}.

are functions of R, by Equation 2 and obtain the normalized numbers as functions of F. With $g(F)$ from Equation 26 we finally obtain the plain expressions

$$T_{\text{total}}(F) = 3F - g(F) \qquad (27)$$

$$U_{\text{dyn}}(F) = +4g(F) \qquad (28)$$

$$U_{\text{static}}(F) = 2[F - g(F)] \qquad (29)$$

$$U_{\text{total}}(F) = 2[F + g(F)] \qquad (30)$$

$$V_{\text{circles}}(F) = (1 - F)^4 \qquad (31)$$

$$V_{\text{arcs}}(F) = +4g(F) \qquad (32)$$

$$V_{\text{total}}(F) = (1 - F)^4 + 4g(F) \qquad (33)$$

$T(F)$, $U(F)$ and $V(F)$ are shown in Figs 10, 12 and 13, respectively.

5.3. Example

Given: 10^5 Poisson-distributed nuclei having arrived at a degree of growth $F = 0.6$.

Wanted: The mean numbers of the ten properties.

In a good approximation we obtain the mean numbers of the:

grain boundaries of type 1

$$10^5 T_{\text{type 1}}(F = 0.6) = 37\,999$$

grain boundaries of type 2

$$10^5 T_{\text{type 2}}(F = 0.6) = 71\,119$$

grain boundaries of type 3

$$10^5 T_{\text{type 3}}(F = 0.6) = 34\,592$$

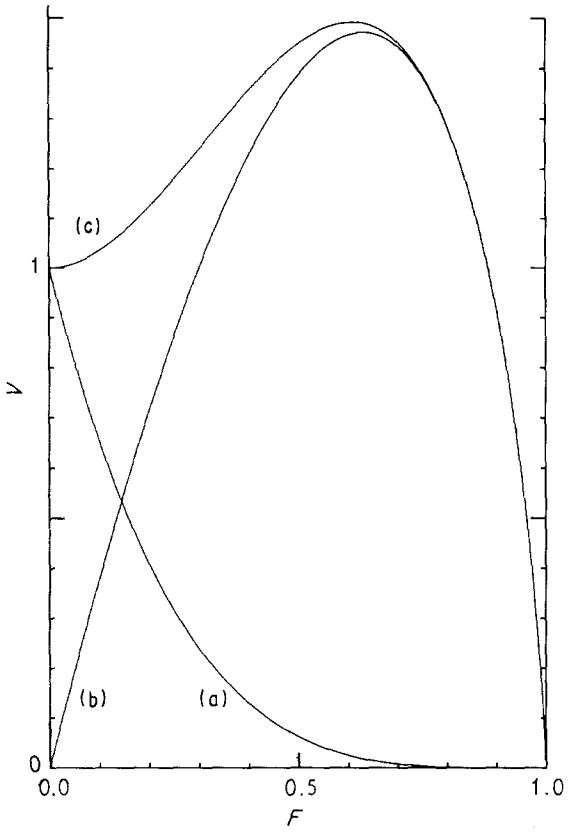

Figure 13 Graph of the normalized numbers of circles, arcs and all growth fronts in dependence on F: (a) V_{circles}, (b) V_{arcs} and (c) V_{total}.

Exact mean numbers are obtained for:

all grain boundaries	$10^5 T_{\text{total}}(F = 0.6)$	= 143 348
dynamic triple points	$10^5 U_{\text{dyn}}(F = 0.6)$	= 146 607
static triple points	$10^5 U_{\text{static}}(F = 0.6)$	= 46 697
all triple points	$10^5 U_{\text{total}}(F = 0.6)$	= 193 303
circles	$10^5 V_{\text{circles}}(F = 0.6)$	= 2560
arcs	$10^5 V_{\text{arcs}}(F = 0.6)$	= 146 607
all growth fronts	$10^5 V_{\text{total}}(F = 0.6)$	= 149 167

6. Computer simulation

Again we chose 10^5 nuclei and $F = 0.6$. We counted the numbers of all ten properties in a computer simulation. The computer simulation was repeated three times in order to even out fluctuations. In the first column of Table II the properties are listed. In the second column the values of the example in Section 5.3 are listed. In the remaining three columns the numbers of the properties were counted by computer simulation.

From Table II it can be seen that within the range of fluctuations the theoretical values are in good agreement with the simulation results.

Appendix: Deduction for static triple points

Three neighbouring growing spherulites meet in one point. This point is the static triple point. The distance to each of the nuclei of the three spherulites is the same, and we denote this distance by r.

The relative number to find three Poisson-distributed nuclei in a distance between r and $r + \varepsilon$, described by the probability $q_3(\Delta S)$, and simultaneously to find no nucleus within the circle with radius r, described by $q_0(S)$, amounts to

$$q(S, \Delta S) = q_3(\Delta S)\, q_0(S) \qquad \text{(A1)}$$

It holds that $S = \pi r^2$ and $\Delta S = 2\pi r\varepsilon$, where ε is infinitesimally small. Therefore according to the Poisson distribution $q(S, \Delta S)$ becomes

$$q(r, \varepsilon) = \frac{(2\pi r\varepsilon)^3}{3!} \exp(-2\pi r\varepsilon) \exp(-\pi r^2)$$

TABLE II $N = 10^5$ and $F = 0.6$

Property	Theory	Counted out by computer simulation		
		1	2	3
Grain boundaries of type 1	37 999	37 948	37 683	38 127
Grain boundaries of type 2	71 119	70 713	70 925	70 794
Grain boundaries of type 3	34 592	34 464	34 471	34 159
Grain boundaries of all types	143 348	143 125	143 079	143 080
Dynamic triple points	146 607	146 610	146 292	147 052
Static triple points	46 697	46 553	46 623	46 376
All triple points	193 303	193 163	192 920	193 428
Circles	2560	2581	2620	2531
Arcs	146 607	146 610	146 292	147 052
All growth fronts	149 167	149 191	148 912	149 583

Because of the infinitesimal size of ε, $\exp(-2\pi r\varepsilon) \approx 1$, and therefore

$$q(r, \varepsilon) = \frac{(2\pi\varepsilon)^3}{3!} r^3 \exp(-\pi r^2) \quad \text{(A2)}$$

In order to eliminate the infinitesimal ε we normalize the $q(r, \varepsilon)$

$$\int_{r=0}^{\infty} q(r, \varepsilon)\,dr = \frac{(2\pi\varepsilon)^3}{3!} \int_{r=0}^{\infty} r^3 \exp(-\pi r^2)\,dr$$

$$= \frac{(2\pi\varepsilon)^3}{3!} \frac{1}{2\pi^2}$$

This yields

$$p(r) = q(r, \varepsilon) \Big/ \int_{r=0}^{\infty} q(r, \varepsilon)\,dr = 2\pi^2 r^3 \exp(-\pi r^2) \quad \text{(A3)}$$

Of course it holds that $\int_{r=0}^{\infty} p(r)\,dr = 1$.

We must integrate $p(r)$ from $r = 0$ to $r = R$ in order to include all static triple points

$$P(R) = \int_{r=0}^{R} p(r)\,dr$$

$$= \int_{r=0}^{R} \pi r^2 \exp(-\pi r^2) 2\pi r\,dr \quad \text{(A4)}$$

The substitution $X = \pi r^2$, which yields $dX = 2\pi r\,dr$, gives as a result

$$P(R) = \int_{X=0}^{\pi R^2} X \exp(-X)\,dX = -(1 + X) \exp(-X) \Big|_{X=0}^{\pi R^2} = 1 - (1 + \pi R^2) \exp(-\pi R^2) \quad \text{(A5)}$$

Because of the normalization $P(R)$ is not the normalized number of static triple points in dependence on R. We saw in Section 3.2 that in the transformed microstructure there are two static triple points for one nucleus. Therefore, Equation A5 yields

$$U_{\text{static}}(R) = 2P(R) = 2[1 - (1 + \pi R^2) \times \exp(-\pi R^2)] \quad \text{(19)}$$

Acknowledgements

We thank Dipl.-Phys. M. Biermann for help with the manuscript and Dr P. Franke for proofreading.

References

1. G. E. W. SCHULZE and H.-P. WILBERT, *J. Mater. Sci. Lett.* **8** (1989) 71.
2. *Idem, ibid.* **10** (1991) 770.
3. A. RÉNYI, "Wahrscheinlichkeitsrechnung" (Deutscher Verlag der Wissenschaften, Berlin, 1977).
4. M. AVRAMI, *J. Chem. Phys.* **8** (1940) 212.
5. G. E. W. SCHULZE and H.-P. WILBERT, *J. Mater. Sci.* **24** (1989) 3101.
6. G. E. W. SCHULZE, L. O. SCHWAN and R. WILLERS, *ibid.* **24** (1989) 3107.
7. J L. MEIJERING, *Philips Res. Rep.* **8** (1953) 270.
8. G. E. W. SCHULZE and L. O. SCHWAN, *Z. Metallkde* **83** (1992) 208.

Received 4 November 1991
and accepted 2 September 1992